

Flow Rate Measurement of Rarefied Binary Gases in Long Rectangular Microchannels

Lajos SZALMAS^{1,2*}, Stéphane COLIN¹, Dimitris VALOUGEORGIS²

* Corresponding author: Tel.: ++33 (0)5 61 55 98 94; Fax: ++33 (0)5 61 55 99 50;

Email: lszalmas@gmail.com, szalmas@insa-toulouse.fr

1 Institut National des Sciences Appliquées de Toulouse, ICA (Institut Clément Ader),
Université de Toulouse, France

2 Department of Mechanical Engineering, University of Thessaly, Greece

Abstract The flow rate of binary gas mixtures through rectangular long microchannels is measured and compared to the numerical solution of the McCormack kinetic model. The microchannels are etched in silicon, and each individual channel has width=21, height=1.15, length=5000 μm . The measurement refers to He/Ar and He/Kr gas mixtures and are based on the constant volume method. The microchannel is placed between an upstream and a downstream reservoir having different pressures. The flow through the microsystem is maintained by the pressure drop between the containers and the flow rate is determined from the pressure variations in the reservoirs. In the case of He/Ar, measurements have been performed for several values of its concentration varying between zero and one, while in the case of He/Kr only a concentration equal to 0.5 is considered. The pressure ratio between the two containers is in the range of 3-7 and the corresponding average Knudsen numbers are in the range of 0.12-0.98. The results of the flow rate measurement are compared to the discrete velocity solution of the McCormack kinetic model and very good agreement between experiment and simulation has been obtained for all flow configurations. The relative discrepancy between the experimental and numerical results is in the range of the experimental uncertainty.

Keywords: Micro flow, Binary gases, Constant volume, McCormack model

1. Introduction

Recently, gaseous flows in micro-scale devices have attracted considerable interest in the scientific community. The increasing interest is well justified by the appearance of new technologies in microfluidics. For these flows, the mean free path between the molecules becomes comparable with the device size, and the flow is considered rarefied. The flow behavior departs from the prediction of the Navier-Stokes equations and the microscopic motion of the molecules needs to be taken into account. The proper description of the gas requires the consideration of the Boltzmann or related kinetic equations. The experimental measurements can be used to determine the flow behavior in these devices and to study various theoretical approaches.

The majority of previous experimental studies refers to flow rate measurement of rarefied gases through different microsystems. The droplet tracking, the constant volume methods and the direct measurement of the pressure drop at constant flow rates have been widely used to deduce the flow rate as a function of the inlet and outlet pressures. Various researchers, including Harley et al. (1995), Arkilic et al. (2001), Zohar et al. (2002), Maurer et al. (2003), Colin et al. (2004), Ewart et al. (2006, 2007) and Marino (2009), have used these techniques to deduce the flow rate. On the basis of the available experimental results, some research groups have also determined the slip coefficients. The above-mentioned studies have focused on single component gases, and only some papers as those of Pitakarnnop et al. (2010) and Szalmas et al. (2010), have been devoted to gaseous mixtures.

For the simulation of gaseous flows, hydrodynamic equations coupled with slip and jump boundary conditions may be applied for small Knudsen numbers (Aubert and Colin, 2001). However, a kinetic description is necessary for the whole range of the gas rarefaction. The discrete velocity methodology has been used to solve various kinetic equations by Sharipov (2002), Graur and Sharipov (2007), Naris et al. (2008), Varoutis et al. (2009) for rectangular, elliptical, triangular and trapezoidal cross sections, respectively. For mixtures, the McCormack model has been solved for channels with circular by Sharipov and Kalempa (2002), rectangular by Naris et al. (2005), triangular and trapezoidal channels by Szalmas and Valougeorgis (2010). Takata and Kosuge (2009) presented results for binary mixtures flowing between two parallel plates. However, currently, there are only a few comparative studies, where the theoretical model is compared to the experimental data.

The present work is devoted to the flow rate measurement of noble gas mixtures in rectangular long microchannels by using the constant volume method. In particular, the gas mixtures of He/Ar and He/Kr are investigated at different flow conditions. The results of the flow rate are compared to the discrete velocity solution of the McCormack kinetic model.

2. Flow configuration

Binary gas mixture flowing through long rectangular microchannels is considered. The channel axis lies in the x coordinate direction, while the cross section is located in the y,z coordinate sheet. An individual microchannel has the following dimensions: width $W=21$, height $H=1.15$, length $L=5000$ micrometers. The mixture has two components $\alpha=1,2$ and $\alpha=1$ refers to the lighter species. The molar masses and the densities of the components are denoted by m_α, n_α . The total molar density is introduced as $n=n_1+n_2$. The molar masses of the gases are given by $m_{He}=4.003\text{g/mol}$, $m_{Ar}=39.95\text{g/mol}$ and $m_{Kr}=83.80\text{g/mol}$. The concentration of the mixture is defined by $C=n_1/n$. The concentration in the upstream reservoirs C_A is used as a reference value to define the problem. The concentration in the downstream reservoir C_B is equal to C_A . The pressure of the gas is denoted by P . Its values in the upstream and downstream reservoirs are given by P_A and P_B . The rarefaction degree of the gas is characterized by the rarefaction parameter

$$\delta = \frac{PH}{\mu(C)v_0(C)} \quad (1)$$

where $\mu(C)$ is the gas viscosity and $v_0(C)$ is the characteristic molecular speed defined by

$$v_0(C) = \sqrt{\frac{2kT}{m}} \quad (2)$$

with k, T denoting the Boltzmann constant, the temperature and $m=Cm_1+(1-C)m_2$ is the average molar mass. The equivalent Knudsen number is introduced by $Kn=1/\delta$. Its mean value in the channel is quantified by $Kn_0=2/(\delta_A+\delta_B)$, where δ_A and δ_B denote the rarefaction parameters in the upstream and downstream reservoirs.

A main interest of the present work is in the component molar flow rates defined by

$$J_\alpha = n_\alpha \int u_{\alpha x} dA, \quad (3)$$

where $u_{\alpha x}$ is the velocity of species α of the mixture in the direction of the channel axis and the integration refers to the cross section of the channel, $A=HW$. The total flow rate of the mixture is defined by $J=J_1+J_2$.

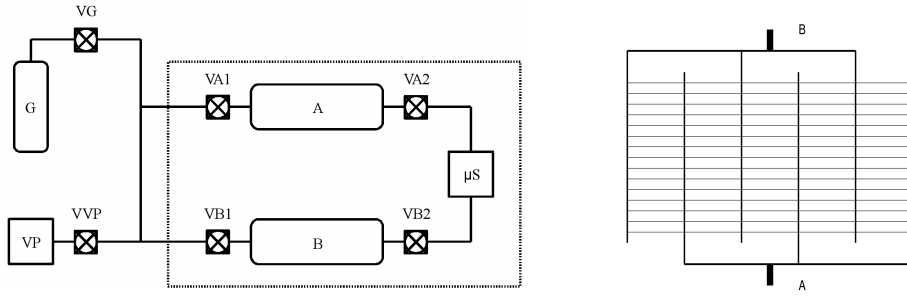


Figure 1. Layout of the flow rate setup (left) and the bunch of microchannels (right).

3. Experimental approach

The measurement is based on the constant volume method. The overall experimental setup, shown in Figure 1 and described in detail in the paper of Pitakarnnop et al. (2010), is located in a plastic chamber kept at isothermal conditions. The temperature is regulated by two Peltier modules. The temperature is accurately measured by four PT100 temperature sensors with accuracy better than 0.1K and fixed at 299.2K. The microsystem (μS) having 380 parallel microchannels is placed between upstream (A) and downstream (B) containers. The inlet and outlet of the system are connected to the reservoirs through valves VA2 and VB2. The pressure in the containers is measured by two Inficon capacitance gauges (CDG025D) with accuracy better than 0.2% during the experiment. The measurement is based on a three-step procedure. In the first step, the system is vacuumed out by a pump (VP); the reservoirs and the microsystem are filled up with the mixture at pressure P_B from an external gas bottle (G). Then, valve VA2 is closed, and the possible outgassing or leakage flow rate, J_{Bo} , is determined from the pressure variation in container B. In the second step, container A is filled up with the gas mixture at pressure P_A , then VA2 is opened allowing the gas flowing through the microsystem. This second step is the actual flow rate measurement, when the total flow rates J_A' and J_B' are determined from the pressure variations in tanks A and B. In the third step, the outlet container and the microsystem are filled up with the mixture at the actual pressure in reservoir A in order to have equal pressure everywhere in the system. Then, valve VB2 is closed and the possible outgassing or leakage flow rate, J_{Ao} , is determined in the inlet container A. The outgassing or leakage flow rates are used to correct the data J_A' and J_B' to yield the final J_A and J_B flow rates. The final total flow rate is then defined by $J = (J_A + J_B)/2$.

The flow rate is deduced from the pressure variation as defined by the state equation of the gas

$$J_{A,B} = \mp \frac{dN_{A,B}}{dt} = \mp \frac{d}{dt} \left(\frac{P_{A,B} V_{A,B}}{R_g T} \right), \quad (4)$$

where $N_{A,B}$ is the molar amount of the molecules in container A or B, $V_A = 1.708 \text{e-}4 \text{m}^3$ and $V_B = 1.685 \text{e-}4 \text{m}^3$ are the volumes of the upstream and downstream containers, $R_g = 8.314 \text{J}/(\text{mol K})$ is the global gas constant and T is the temperature. From Eq. (4), the flow rate is obtained by

$$J_{A,B} = \mp \frac{V_{A,B}}{R_g T} \frac{dP_{A,B}}{dt} \left(1 - \frac{dT/T}{dP_{A,B}/P_{A,B}} \right). \quad (5)$$

The relative temperature and pressure variations in the experiments are in the order of $dT/T = 4 \times 10^{-4}$ and $dP_{A,B}/P_{A,B} = 2 \times 10^{-2}$. As a consequence, the flow rate can be written by

$$J_{A,B} = \mp \frac{V_{A,B}}{R_g T} a_{A,B} c_{A,B}, \quad (6)$$

where the quantity $a_{A,B}$ is the time derivative of the pressure variation $P_{A,B}(t)=a_{A,B}t+b_{A,B}$, and $c_{A,B}=(1-(dT/T)/(dP_{A,B}/P_{A,B}))=1\pm 0.02$. The uncertainty of $a_{A,B}$ is $\pm 0.5\%$. The total uncertainty of the experiment consists of the uncertainty of $V_{A,B}$, T and the coefficients $a_{A,B}$ and $c_{A,B}$ such that

$$\frac{\Delta J_{A,B}}{J_{A,B}} = \frac{\Delta V_{A,B}}{V_{A,B}} + \frac{\Delta T}{T} + \frac{\Delta a_{A,B}}{a_{A,B}} + \frac{\Delta c_{A,B}}{c_{A,B}} = \pm(1.3\% + 0.2\% + 0.5\% + 2\%) = \pm 4\%. \quad (7)$$

4. Computational approach

The McCormack linearized kinetic model is used to describe the flow. Since the length of the channel is much larger than its height, end effects are neglected. Also, the velocity of the gas is small compared to the characteristic molecular speed and this justifies the usage of the linearized description. The calculation of the flow rate involves two steps. First, the local quantities of the flow, the so-called kinetic coefficients, are calculated and then the global flow quantities, such as the flow rate, are deduced (Szalmas et al., 2010).

For the kinetic calculation, two thermodynamic fluxes are introduced

$$J_P = -\int (n_1 u_{1x} + n_2 u_{2x}) dA, \quad J_C = -n_1 \int (u_{1x} - u_{2x}) dA. \quad (8)$$

These fluxes are connected to the local pressure and concentration gradients defined by

$$X_P = \frac{\partial P}{\partial x} \frac{H}{P}, \quad X_C = \frac{\partial C}{\partial x} \frac{H}{C} \quad (9)$$

such that

$$J_P = \frac{nAv_0}{2} (A_{PP} X_P + A_{PC} X_C), \quad J_C = \frac{nAv_0}{2} (A_{CP} X_P + A_{CC} X_C). \quad (10)$$

As a consequence, the fluxes are linear functions of the X_P and X_C gradients, which drive the flow through the channel. The McCormack model is solved to obtain the so-called kinetic coefficient $A_{PP}, A_{PC}, A_{CP}, A_{CC}$ in the whole range of the gas concentration and rarefaction by using the realistic potential developed by Kestin et al. (2002). The McCormack model is solved by the discrete velocity method with a computational grid consisting of 201x201 nodes for $\delta \leq 1$ and 301x301 nodes for $\delta > 1$ in the physical space and of 64 magnitudes and 280 polar angles for the whole range of the gas rarefaction.

The component flow rates can be expressed in terms of the thermodynamic fluxes such that

$$J_1 = -CJ_P - (1-C)J_C, \quad J_2 = -(1-C)(J_P - J_C). \quad (11)$$

It is noted that the flow rates of the species are constant along the channel axis at every cross section because of the conservation of the molecular number. By using this latter relationship, the expression of J_P, J_C as a function of X_P, X_C and the ideal gas law, the component flow rates can be expressed in terms of the local pressure and concentration gradients such that

$$J_1 = -\frac{PAH}{mvL} \left[(CA_{PP} - (1-C)A_{CP}) \frac{\partial P}{\partial x'} \frac{1}{P} + (CA_{PC} + (1-C)A_{CC}) \frac{\partial C}{\partial x'} \frac{1}{C} \right], \quad (12)$$

$$J_2 = -\frac{PAH}{mvL} (1-C) \left[(A_{PP} - A_{CP}) \frac{\partial P}{\partial x'} \frac{1}{P} + (A_{PC} - A_{CC}) \frac{\partial C}{\partial x'} \frac{1}{C} \right], \quad (13)$$

where $x'=x/L$ is the dimensionless spatial variable along the channel axis. Eqs. (12)-(13) constitute a

Table 1. Flow rates through 380 parallel microchannels for He/Ar and He/Kr mixtures for outlet pressure $P_B=15.2\text{kPa}$.

Mixture	C_A	$P_A(\text{Pa})$	$P_B(\text{Pa})$	P_A/P_B	Kn_0	$J_{exp}(\text{mol/s})$	$\Delta_{exp}(\%)$	$J_{comp}(\text{mol/s})$	$\Delta(\%)$
He/Ar	0.0	45908	15200	3.02	0.23	8.55E-9	-1.02	8.54E-9	-0.03
		59198	15200	3.89	0.19	1.34E-8	-3.69	1.31E-8	-2.12
		73582	15200	4.84	0.16	1.86E-8	-0.45	1.88E-8	0.86
		89571	15200	5.89	0.13	2.68E-8	-3.45	2.58E-8	-3.94
		104238	15200	6.86	0.12	3.39E-8	-0.62	3.30E-8	-2.65
	0.1017	45809	15201	3.01	0.24	9.00E-9	-2.84	9.12E-9	1.31
		59232	15200	3.90	0.20	1.42E-8	1.01	1.40E-8	-1.56
		73603	15200	4.84	0.17	1.95E-8	-0.06	1.98E-8	1.47
		89424	15199	5.88	0.14	2.73E-8	-2.52	2.69E-8	-1.26
		104225	15202	6.86	0.12	3.53E-8	-0.67	3.44E-8	-2.82
	0.3012	44327	15199	2.92	0.28	9.75E-9	-2.27	1.00E-8	2.62
		59292	15200	3.90	0.23	1.63E-8	-3.43	1.59E-8	-2.27
		74553	15200	4.90	0.19	2.35E-8	-0.28	2.26E-8	-3.88
		89629	15200	5.90	0.16	3.05E-8	-3.43	2.99E-8	-2.12
		104034	15200	6.84	0.14	3.74E-8	-0.22	3.75E-8	0.47
	0.5010	45217	15200	2.97	0.33	1.18E-8	-2.51	1.22E-8	3.93
		60197	15201	3.96	0.26	1.83E-8	-1.81	1.89E-8	3.23
		74279	15201	4.89	0.22	2.51E-8	0.27	2.58E-8	2.90
		89125	15200	5.86	0.19	3.40E-8	-1.13	3.37E-8	-1.09
		104034	15200	6.84	0.16	4.25E-8	-1.26	4.22E-8	-0.80
	0.7019	45823	15200	3.01	0.39	1.46E-8	-3.36	1.52E-8	3.72
		59504	15200	3.91	0.32	2.18E-8	-2.61	2.24E-8	2.53
		74071	15200	4.87	0.27	3.00E-8	-2.11	3.06E-8	1.99
		89356	15200	5.88	0.23	3.84E-8	-1.63	3.98E-8	3.72
		104103	15200	6.85	0.20	4.89E-8	-2.57	4.94E-8	1.05
	0.9014	45671	15199	3.00	0.51	1.85E-8	-3.74	1.92E-8	3.80
		59550	15200	3.92	0.42	2.74E-8	-0.18	2.84E-8	3.35
		74267	15199	4.89	0.35	3.86E-8	-2.67	3.87E-8	0.20
		90106	15200	5.93	0.29	5.21E-8	-0.52	5.04E-8	-3.27
		104329	15201	6.86	0.26	6.19E-8	-2.63	6.17E-8	-0.19
	1.0	45673	15200	3.00	0.64	2.17E-8	0.87	2.21E-8	1.79
		59241	15200	3.90	0.52	3.32E-8	-3.35	3.26E-8	-1.99
		74048	15200	4.87	0.43	4.54E-8	-1.29	4.47E-8	-1.67
		89282	15200	5.87	0.37	5.97E-8	-3.67	5.79E-8	-3.07
		103915	15200	6.84	0.33	7.34E-8	-2.91	7.13E-8	-2.86
He/Kr	0.5010	45278	15199	2.98	0.26	9.73E-9	-3.08	1.01E-8	3.19
		59797	15200	3.93	0.21	1.54E-8	-0.59	1.54E-8	-0.44
		73618	15204	4.84	0.18	2.13E-8	-3.56	2.08E-8	-2.40
		87696	15201	5.77	0.15	2.73E-8	-3.03	2.68E-8	-1.83
		104033	15200	6.84	0.13	3.52E-8	-3.46	3.45E-8	-2.02

system of two ordinary differential equations, which is supplemented with the boundary condition for the pressure and the concentration at the channel inlet and outlet

$$P(0)=P_A, \quad P(1)=P_B, \quad C(0)=C_A, \quad C(1)=C_B. \quad (14)$$

Eqs. (12)-(13) together with the boundary conditions are numerically solved to yield the component flow rates and the pressure and concentration distributions. The solution is carried out by discretizing the x' coordinate with grid resolution 1/500 and using the Euler method.

5. Results

The flow rates of He/Ar and He/Kr noble gas mixtures are measured. Two downstream pressures $P_B=15.2\text{kPa}$ and 8kPa are investigated. The flow rates are compared to the kinetic calculation. The flow rate for the total 380 parallel microchannels is deduced.

Table 1 shows the results for outlet pressure $P_B=15.2\text{kPa}$. Results are tabulated for the He/Ar mixture with concentration values $C_A=[0.1017;0.3012;0.5010;0.7019;0.9014]$ including the single

Table 2. Flow rates through 380 parallel microchannels for He/Ar and He/Kr mixtures for outlet pressure $P_B=8\text{kPa}$.

Mixture	C_A	$P_A(\text{Pa})$	$P_B(\text{Pa})$	P_A/P_B	Kn_0	$J_{exp}(\text{mol/s})$	$\Delta_{exp}(\%)$	$J_{comp}(\text{mol/s})$	$\Delta(\%)$
He/Ar	0.0	31822	8000	3.98	0.35	6.07E-9	3.14	5.93E-9	-2.28
		40113	8000	5.01	0.29	8.63E-9	1.44	8.37E-9	-3.17
		47964	8000	6.00	0.25	1.13E-8	-1.80	1.09E-8	-3.88
		55969	8002	6.99	0.22	1.31E-8	-3.78	1.36E-8	3.55
	0.1017	31989	8000	4.00	0.37	6.36E-9	-3.04	6.55E-9	2.85
		40346	8000	5.04	0.31	9.28E-9	-1.76	9.14E-9	-1.55
		47949	8000	5.99	0.27	1.17E-8	-1.48	1.17E-8	-0.20
		56125	8000	7.02	0.23	1.47E-8	-1.86	1.46E-8	-0.85
	0.3012	31977	8000	4.00	0.42	7.69E-9	-2.76	7.86E-9	2.10
		40290	8000	5.04	0.35	1.07E-8	1.26	1.08E-8	1.00
		47968	8000	6.00	0.30	1.32E-8	-3.39	1.36E-8	3.23
		56000	8000	7.00	0.26	1.66E-8	-3.29	1.67E-8	0.41
	0.5010	31781	7997	3.97	0.49	9.48E-9	-3.11	9.46E-9	-0.18
		40109	8000	5.01	0.41	1.23E-8	-3.52	1.28E-8	3.85
		47854	8000	5.98	0.35	1.55E-8	-1.04	1.61E-8	3.70
		55934	8000	6.99	0.31	1.90E-8	-1.45	1.96E-8	2.84
	0.7019	31909	8000	3.99	0.60	1.15E-8	-3.41	1.18E-8	2.70
		40266	8001	5.03	0.49	1.52E-8	-3.97	1.58E-8	3.95
		48003	8000	6.00	0.42	1.92E-8	-2.38	1.97E-8	2.96
		55984	8000	7.00	0.37	2.33E-8	-3.21	2.39E-8	2.64
	0.9014	31947	8000	3.99	0.78	1.47E-8	-3.18	1.50E-8	2.22
		40176	8000	5.02	0.64	2.00E-8	-3.15	2.05E-8	2.29
		47888	8000	5.99	0.56	2.50E-8	-1.25	2.50E-8	0.17
		55820	8000	6.98	0.49	2.95E-8	1.17	3.03E-8	2.55
	1.0	31691	8000	3.96	0.98	1.68E-8	-2.19	1.69E-8	0.86
		40047	8000	5.01	0.81	2.39E-8	-1.36	2.31E-8	-3.50
		47739	8000	5.97	0.70	2.91E-8	0.50	2.88E-8	-0.91
		55917	8000	6.99	0.61	3.62E-8	3.43	3.51E-8	-3.00
He/Kr	0.5010	31914	8000	3.99	0.40	7.91E-9	2.40	7.87E-9	-0.54
		40232	8000	5.03	0.33	1.02E-8	-3.67	1.06E-8	3.27
		48055	8000	6.01	0.28	1.28E-8	-3.40	1.32E-8	3.02
		55928	8000	6.99	0.25	1.63E-8	0.67	1.60E-8	-2.03

Table 3. Comparison between the McCormack and equivalent single gas flow rates for $P_B=15.2\text{kPa}$ and $C_A=0.5010$.

He/Ar				He/Kr			
P_A/P_B	$J_{McC}(\text{mol/s})$	$J_{single}(\text{mol/s})$	$\Delta_s(\%)$	P_A/P_B	$J_{McC}(\text{mol/s})$	$J_{single}(\text{mol/s})$	$\Delta_s(\%)$
2.97	1.22E-8	1.02E-8	16.3	2.98	1.01E-8	7.68E-9	23.6
3.96	1.89E-8	1.63E-8	14.0	3.93	1.54E-8	1.22E-8	20.4
4.89	2.58E-8	2.26E-8	12.5	4.84	2.08E-8	1.71E-8	17.9
5.86	3.37E-8	2.99E-8	11.1	5.77	2.68E-8	2.25E-8	15.9
6.84	4.22E-8	3.79E-8	10.0	6.84	3.45E-8	2.96E-8	14.2

component gas cases, i.e., $C_A=[0.0;1.0]$ and for the He/Kr mixture with concentration value $C_A=0.5010$. The experimental flow rates and kinetic results are presented in the 7th and the 9th columns of the table. The difference between the inlet and the outlet experimental flow rates defined by $\Delta_{exp}=100(1-J_A/J_B)$ is presented in the 8th column. It is shown that the difference is in the range of the experimental uncertainty, which justifies that eventual outgassing or leakage effects are correctly taken into account by the three-step experimental procedure. The comparison between the experimental and kinetic results is quantified by $\Delta=100(1-J_{exp}/J_{comp})$ and shown in the last column of the table. It is clearly seen that there is a good agreement between experiment and simulation, and the deviation is less than the experimental uncertainty in all situations. The flow rate monotonically increases with decreasing concentration because the portion of the faster He is larger at smaller concentration. The molar flow rates of He/Kr are always smaller compared to the corresponding ones of He/Ar and this is justified by the larger molecular mass of Kr than that of Ar, taking into

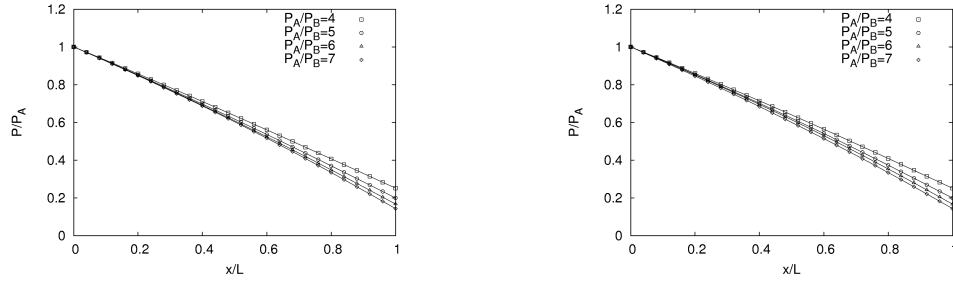


Figure 2. Pressure distribution along the channel for He/Ar (left) and He/Kr (right) mixtures at downstream pressure 8kPa and concentration $C_A=0.5010$.

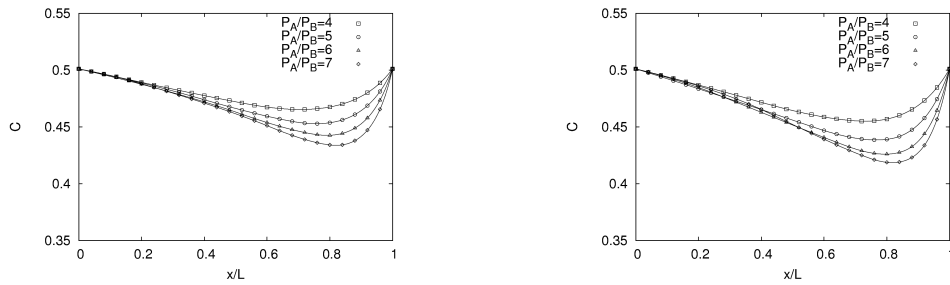


Figure 3. Concentration distribution along the channel for He/Ar (left) and He/Kr (right) mixtures at downstream pressure 8kPa and concentration $C_A=0.5010$.

account that heavier molecules possess smaller velocities.

Table 2 shows the corresponding results for downstream pressure $P_B=8\text{kPa}$. The results are presented for the same concentration values as for $P_B=15.2\text{kPa}$. Again, very good agreement between the experimental and kinetic results is found. The discrepancy is less than the experimental uncertainty. Comparing the two tables, it can be concluded that the flow rates are smaller in Table 2. This situation occurs because the inlet and outlet pressures are smaller, though the pressure ratio is the same, which results into smaller gas density and flow rates.

In Table 3, the McCormack results for $P_B=15.2\text{kPa}$ and $C_A=0.5010$ are compared to the equivalent single gas flow rates computed with the mixture viscosity and the average mass. Specifically, the equivalent single gas, substituting the He/Ar mixture, has $\mu=2.37\text{e-}5\text{Pa}\cdot\text{s}$ and $m=21.9\text{g/mol}$, while the corresponding values in the He/Kr case are $2.70\text{e-}5\text{Pa}\cdot\text{s}$ and 43.8g/mol . The discrepancy between the results is quantified by $\Delta_s=100(1-J_{\text{single}}/J_{\text{McC}})$. The differences vary from 10.0% up to 23.6% and it is clearly seen that the discrepancy is increased i) as the mass ratio of the light over the heavy gas is decreased and ii) as the Knudsen number is increased.

The typical pressure and concentration curves are shown in Figures 2 and 3 for the two mixtures for concentration $C_A=0.5010$ at downstream pressure $P_B=8\text{kPa}$. The pressure profiles on Figure 2 are in accordance with the pressure ratios, and they are nearly linear functions of the coordinate along the channel axis. This situation occurs because the Knudsen number is relatively large, and the pressure profile is linear due to opposite effects of rarefaction and compressibility on the pressure gradient. In Figure 3, the concentration distributions are non-uniform, which indicates the existence of the separation phenomena in the microchannel. The deviation of the concentration with the reservoir concentration increases with increasing pressure ratio. In addition, the He/Kr mixture exhibits larger concentration drop than the He/Ar mixture. The reason of this behavior is the larger mass difference between the components for the He/Kr mixture.

6. Conclusions

The flow rate of He/Ar and He/Kr mixtures are measured through long rectangular microchannels, and the experimental results are compared to the kinetic calculation on the basis of the McCormack model. A good agreement between the two approaches is obtained in all cases. Representative curves of the pressure and concentration distributions are provided. The mixtures exhibit the separation phenomena, which is stronger for the He/Kr mixture having larger molecular mass ratio. The comparative study indicates that the McCormack kinetic model is a valuable tool for describing pressure driven gaseous mixtures in the considered parameter range. It has been also found that in order to have accurate results the binary mixture can not be approximated as an equivalent single gas with average properties.

Acknowledgment

The research leading to these results has received funding from the European Community's Seventh Framework Programme (FP7/2007-2013) under grant agreement no 215504.

References

1. Arkilic, E.B, Breuer, K.S. and Schmidt, M.A., 2001. Mass flow and tangential momentum accommodation in silicon micromachined channels, *J. Fluid Mech.* 437, 29-43.
2. Aubert, C. and Colin S., 2001. High-order boundary conditions for gaseous flows in rectangular microchannels, *Microscale Thermophys. Eng.* 5, 41-54.
3. Colin, S., Lalonde, P. and Caen, R., 2004. Validation of a second-order slip flow model in rectangular microchannels, *Heat Transfer Eng.* 25, 23-30.
4. Ewart, T., Perrier, P., Graur, I. and Meolans, J.G., 2006. Mass flow rate measurements in gas micro flows, *Exp. Fluids* 41, 487-498.
5. Ewart, T., Perrier, P., Graur, I. and Meolans, J.G., 2007. Mass flow rate measurements in a microchannel, from hydrodynamic to near free molecular regimes, *J. Fluid Mech.* 584, 337-356.
6. Graur, I. and Sharipov, F., 2007. Gas flow through an elliptical tube over the whole range of the gas rarefaction, *Eur. J. Mech. B/Fluids* 27, 335-345.
7. Harley, J.C., Huang, Y.Y., Bau, H.H. and Zemel, J.N., 1995. Gas flow in micro-channels, *J. Fluid Mech.* 284, 257-274.
8. Kestin, J., Knierim, K., Mason, E.A., Najafi, B., Ro, S.T., Waldman, M., 1984. Equilibrium and transport properties of the noble gases and their mixture at low densities. *J. Phys. Chem. Ref. Data*, 13, 229-303.
9. Marino, L., 2009. Experiments on rarefied gas flows through tubes, *Microfluid. Nanofluid.* 6, 109-119.
10. Maurer, J., Tabeling, P., Joseph P. and Willaime, H., 2003. Second-order slip laws in microchannels for helium and nitrogen, *Phys. Fluids* 15, 2613-2621.
11. Naris, S. and Valougeorgis, D., 2008. Rarefied gas flow in a triangular duct based on a boundary fitted lattice, *Eur. J. Mech. B/Fluids* 27, 810-822.
12. Naris, S., Valougeorgis, D., Sharipov, F. and Kalempa, D., 2005. Flow of gaseous mixtures through rectangular microchannels driven by pressure, temperature and concentration gradients, *Phys. Fluids* 17, 100607.1-12.
13. Pitakarnnop, J., Varoutis, S., Valougeorgis, D., Geoffroy, S., Baldas, L. and Colin, S., 2010. A novel experimental setup for gas microflows, *Microfluid. Nanofluid.* 8, 57-72.
14. Sharipov, F., 2002. Rarefied gas flow through a long rectangular channel, *J. Vac. Sci. Technol. A* 17, 3062-3066.

15. Sharipov, F., Kalempa, D., 2002. Gaseous mixture flow through a long tube at arbitrary Knudsen numbers, *J. Vac. Sci. Technol. A* 20, 814-822.
16. Szalmas, L., Pitakarnnop, J., Geoffroy, S, Colin, S. and Valougeorgis, D., 2010. Comparative study between computational and experimental results for binary rarefied gas flows through long microchannels, *Microfluid. Nanofluid.* 9, 1103-1114.
17. Szalmas, L. and Valougeorgis, D., 2010. Rarefied gas flow of binary mixtures through long channels with triangular and trapezoidal cross sections, *Microfluid. Nanofluid.* 9, 471-487.
18. Takata, S and Kosuge, S., 2009. Database for flows of binary gas mixtures through a plane microchannel, *Eur. J. Mech. B/Fluids* 28, 170–184.
19. Varoutis, S., Naris, S., Hauer, V., Day, C. and Valougeorgis, D., 2009. Experimental and computational investigation of gas flows through long channels of various cross sections in the whole range of the Knudsen number, *J. Vac. Sci. Technol.* 27, 89-100.
20. Zohar, Y, Lee, S.Y.K., Lee, W.Y., Jiang, L. and Tong, P., 2002. Subsonic gas flow in a straight and uniform microchannel, *J. Fluid Mech.* 472, 125-151.